The inter-annual variability of tropical precipitation and inter-hemispheric energy transport

Aaron Donohoe *

Massachusetts Institute of Technology, Cambridge, Massachusetts

John Marshall, David Ferreira, Kyle Armour, and David McGee

(Manuscript submitted January 10, 2014)

* *Corresponding author address:* Aaron Donohoe, Massachusetts Institute of Technology, Dept. of Earth, Atmospheric and Planetary Sciences, Room Number 54-918, 77 Massachusetts Avenue, Cambridge, MA 02139-4307.

E-mail: thedhoe@mit.edu

ABSTRACT

The inter-annual variability of the location of the inter-tropical convergence zone (ITCZ) is strongly (R=0.75) correlated with the atmospheric heat transport across the equator (AHT_{EQ}) over the satellite era (1979-2009). A 1° northward displacement of the ITCZ is associated with 0.34 PW of anomalous AHT_{EQ} from north to south. The AHT_{EQ} and precipitation anomalies are both associated with an intensification of the climatological Hadley cell which is displaced north of the equator. This relationship suggests that the tropical precipitation variability is driven by a hemispheric asymmetry of energy input to the atmosphere at all latitudes by way of the constraint that AHT_{EQ} is balanced by a hemispheric asymmetry in energy input to the atmosphere.

A 500 year coupled model simulation also features strong inter-annual correlations between the ITCZ location and AHT_{EQ}. The inter-annual variability of AHT_{EQ} in the model is associated with a hemispheric asymmetry in top of the atmosphere radiative anomalies in the tropics with the northern hemisphere gaining energy when the ITCZ is displaced northward. The surface heat fluxes make a secondary contribution to the inter-annual variability of AHT_{EQ} despite the fact that the inter-annual variability of the ocean heat transport across the equator (OHT_{EQ}) is comparable in magnitude to that in AHT_{EQ}. The OHT_{EQ} makes a minimal impact on the atmospheric energy budget because the vast majority of the inter-annual variability in OHT_{EQ} is stored in the sub-surface ocean and, thus, the inter-annual variability of OHT_{EQ} does not strongly impact the atmospheric circulation.

1. Introduction

The region of intense tropical precipitation, known as the intertropical convergence zone (ITCZ), is co-located with the ascending branch of the Hadley cell (Hadley 1735). The atmospheric heat transport in the deep tropics is dominated by the mean overturning circulation, with net heat transport oriented in the direction of motion in the upper branch of the Hadley cell (Held 2001). Therefore, energy is transported away from the ITCZ. Consequently, an ITCZ in the Southern Hemisphere (SH) implies northward atmospheric energy transport across the equator ($\equiv \mathrm{AHT}_{EQ}$), and an ITCZ in the Northern Hemisphere (NH) requires southward AHT_{EQ} (Frierson and Hwang 2012).

The close connection between ITCZ location and AHT_{EQ} has been well documented in the recent literature, across a myriad of timescales and applications ranging from idealized model simulations to the observational data. Zhang and Delworth (2005) found that freshwater hosing in the North Atlantic resulted in a shutdown of the Atlantic meridional overturning circulation, cooling the NH and shifting the ITCZ to the south. They related the ITCZ shift to the enhanced northward AHT_{EQ} demanded by the system as the northward ocean heat transport was reduced. Similarly, Yoshimori and Broccoli (2008, 2009); Kang et al. (2008); Chiang and Bitz (2005) found that a prescribed hemispheric asymmetry in forcing (i.e. surface fluxes and ice cover) resulted in an ITCZ shift toward the source of atmospheric heating in order to provide the necessary anomalous AHT_{EQ} away from the heat source.

The climatological mean ITCZ location can be related to the hemispheric asymmetry of energy input into the atmosphere, driven by hemispheric asymmetries in energy fluxes at both the top of the atmosphere (TOA) and at the ocean surface. The resulting AHT_{EQ} requires the ITCZ be located in the hemisphere in which the atmosphere is heated more strongly (Frierson et al. 2013) and the displacement of the ITCZ from the equator is proportional to the magnitude of the hemispheric asymmetry in atmospheric heating (Donohoe et al. 2013). Using this framework, Frierson et al. (2013) and Marshall et al. (2013) recently demonstrated that the observed annual mean ITCZ location (to the north of the equator) is a consequence of northward ocean heat transport across the equator and largely compensating southward AHT_{EQ} demanded by nearly hemispherically symmetric net radiation at the TOA. Moreover, Frierson and Hwang (2012) found that the response of the ITCZ to anthropogenic forcing varies drastically between different global climate models and is strongly correlated with the AHT_{EQ} change demanded by the hemispheric asymmetry in extratropical radiative feedbacks. In this view, the annual mean spatial distribution of tropical precipitation is fundamentally set by the large-scale oceanic circulations (that give rise to the cross-equatorial oceanic energy transport) and the hemispheric asymmetry in TOA energy fluxes.

A quantitative relationship between the ITCZ location and AHT_{EQ} of 3° latitude per PW was established by Donohoe et al. (2013); this scaling was found to apply to the seasonal cycle in the observations, the seasonal cycle in coupled climate models, and the shift in the annual mean ITCZ location due to anthropogenic and paleoclimate forcing. Seasonal variations in AHT_{EQ} (and therefore ITCZ location) are driven by seasonal variations in insolation and opposed by ocean heat storage and emitted radiation at the TOA (Donohoe and Battisti 2013). On seasonal timescales, ocean heat transport and atmospheric energy storage make a negligible contribution to the hemispheric asymmetry of atmospheric heating when compared with the contributions from TOA radiation and ocean energy storage. This is in contrast to the annual mean climatology where ocean heat transport plays a fundamental role in sustaining the mean position of the ITCZ.

Here, we consider the relationship between inter-annual variability in ITCZ location and AHT_{EQ} with a focus on the inter-annual frequency (period of $2 \rightarrow 10$ years) variability. We first quantify this relationship within the observational record, and compare it to the scaling identified previously within the contexts of the seasonal cycle and the equilibrium response to a climate perturbation. We then assess the roles of several candidate mechanisms for driving the inter-annual variability of AHT_{EQ}. As summarized above, in the long-term mean AHT_{EQ} (and thus ITCZ location) is driven primarily by the hemispheric asymmetry of surface heat fluxes via the cross-equatorial ocean heat transport, while over the seasonal cycle it is driven by radiative fluxes at the TOA. A key question is: are anomalies in surface heat fluxes or TOA radiative fluxes responsible for the inter-annual variability of AHT_{EQ} and ITCZ location? Alternatively, are other mechanisms—such as tropical TOA radiative anomalies associated with the shifting Hadley cell itself—of central importance? Distinguishing between these candidate mechanisms for driving inter-annual variability in AHT_{EQ} is difficult in the observational record due to the large uncertainties in estimates of TOA radiation and surface heat fluxes, neither of which are directly observed by a consistent observational network over a prolonged time period (Trenberth and Caron 2001). For this reason, we turn to a coupled atmosphere-ocean general circulation model simulation that also exhibits a strong correlation between ITCZ location and AHT_{EQ} to diagnose the cause of their respective inter-annual variabilities.

Our manuscript is organized as follows. In Section 2 we analyze the observed inter-annual variability of ITCZ location and AHT_{EQ} and the associated anomalies in the tropical precipitation and the Hadley cell. We find that ITCZ location and AHT_{EQ} are strongly correlated over the observational record with a quantitative relationship similar to that identified previously in Donohoe et al. (2013) over seasonal and climatological timescales. We then diagnose a coupled model simulation performed with the Geophysical Fluid Dynamics Laboratory's (GFDL) CM2.1 model (Section 3). We demonstrate that the inter-annual variability of ITCZ location and AHT_{EQ} are strongly correlated in the model (Section 3a), and we partition the inter-annual variability of AHT_{EQ} between radiative anomalies at the TOA and surface heat flux anomalies (Section 3b). We show that the inter-annual variability of AHT_{EQ} is associated with a positive feedback between the ITCZ shift and the cloud radiative response in the tropics. Anomalies in the surface heat fluxes play a secondary role and are uncorrelated with anomalies in ocean heat transport on decadal and shorter timescales. The latter result implies that inter-annual to decadal oscillations in the Atlantic meridional overturning circulation (AMOC) and other ocean circulations do not significantly impact the large scale tropical precipitation. Anomalies in ocean heat transport are largely compensated by energy storage at depth, away from the ocean surface, and thus do not drive corresponding anomalies in atmospheric heat transport at the decadal frequency (Section 3c). A summary and conclusion follows.

2. Observations

In this section, we demonstrate that the inter-annual variability of ITCZ location is negatively correlated with AHT_{EQ} over the satellite era of observations (1979-2009), where the sign of the correlation is defined such that the displacement of the ITCZ to the north is accompanied by anomalous AHT_{EQ} to the south. The inter-annual northward migration of the zonal mean ITCZ is primarily due to an amplification of the climatological maximum precipitation and is accompanied by an amplification of the climatological annual mean Hadley circulation. The associated southward AHT_{EQ} anomaly is due to the intensification of the counter-clockwise rotating Hadley cell at the equator.

a. Data sets and methods

(i) Precipitation and ITCZ location

We analyze monthly mean precipitation data from the National Oceanographic and Atmospheric Administration's Climate Prediction Center's (NOAA CPC) merged analysis (Xie and Arkin 1996) over the period 1979-2009. This gridded data set is derived from gauge measurements, satellite observations, and numerical models. The location of the ITCZ is defined as the precipitation centroid (P_{CENT}) as used by Frierson and Hwang (2012) and Donohoe et al. (2013). P_{CENT} is defined as the median of the zonal average precipitation between 20°S to 20°N. This definition of the ITCZ takes into account the spatial distribution of precipitation over the entire tropics: if the precipitation is strongly peaked (i.e., a delta function), P_{CENT} is co-located with the precipitation maximum; if the precipitation is spatially invariant over the tropics, P_{CENT} is on the equator; if the precipitation is bi-modal, P_{CENT} is a weighted average between the modes.

(ii) Atmospheric heat transport across the equator

The atmospheric heat transport is calculated from National Centers for Environmental Prediction (NCEP) reanalysis fields (Kalnay et al. 1996). We use the four times daily reanalysis with a (horizontal) spectral resolution of T62 and 17 vertical levels. The mass budget is balanced using a barotropic wind correction (Trenberth 1997) prior to the energy flux calculations. The atmospheric energy flux is calculated as the vertical integral of meridional flux of moist static energy (MSE)[1]. This procedure is used to compose monthly averaged atmospheric heat transport from 1979 to 2009.

The atmospheric heat transport is decomposed into components associated with the time and zonal mean circulation, stationary eddies, and transient eddies following Priestley (1948) and Lorenz (1953):

$$AHT = \frac{2\pi a}{g}\int_{P_S}^{0} \underbrace{\left[\overline{V}\right]\left[\overline{MSE}\right]}_{MOC} + \underbrace{\overline{[V]'\,[MSE]'}}_{TOC} + \underbrace{\left[\overline{V}^{*}\;\;\overline{MSE}^{*}\right]}_{Stat.\ eddy} + \underbrace{\left[\overline{V^{*\prime}MSE^{*\prime}}\right]}_{Trans.\ eddy}\; dP\ . \tag{1}$$

V is the meridional velocity. $\overline{Overbars}$ are time averages, [square brackets] are zonal averages, primes (') are departures from the time mean and asterisks (*) are departures from the zonal average. The first term is the energy transport due to the time and zonal average meridional overturning circulation (MOC; i.e., the Hadley cell). The second term is the energy transport due to the temporal covariance of the zonal average overturning circulation and vertical stratification and will be referred as the transient overturning circulation (TOC). The time average vertical stratification ($\left[\overline{MSE}\right]$) is two orders of magnitude larger than the temporal departures in the vertical stratification ($[MSE]'$). Therefore, the TOC energy transport is

[1]Moist static energy is the sum of sensible, latent, and potential energy ($c_pT + Lq + gZ$).

much smaller than that of the MOC and the TOC will be included with the MOC for the remainder of this study. The third term is the stationary eddy energy transport. The fourth term is the transient eddy energy transport.

b. Results

The monthly anomalies in P_{CENT} have a standard deviation of 0.8°, while those in AHT_{EQ} have a standard deviation ($\equiv \sigma$) of 0.3 PW (thin red and blue lines, respectively, in Figure 1a). Monthly anomalies in P_{CENT} and AHT_{EQ} are significantly negatively correlated (R=-0.5) at the 99% confidence interval with a regression coefficient ($\equiv$ b) of -1.5$\pm$ 0.7° PW^{-1} (Figure 1b) where the confidence interval is the 95%. Anomalies in P_{CENT} and AHT_{EQ} are more strongly correlated at lower frequencies; a portion of the high frequency variability in tropical precipitation is not associated with changes in the Hadley cell and, thus, has no associated atmospheric heat transport anomaly. For this reason, we focus here on the variability of tropical precipitation and atmospheric heat transport at the inter-annual frequency. Low pass filtering the monthly anomalies in AHT_{EQ} and P_{CENT} with a 2 year period cutoff filter (thick lines in Figure 1a) results in a correlation coefficient of -0.75 and a regression coefficient of -1.6 $\pm$ 0.7 ° PW^{-1}. The regression coefficient between inter-annual variations in P_{CENT} and AHT_{EQ} is comparable in magnitude to that found over the climatological seasonal cycle (-2.7 $\pm$ 0.6 ° PW^{-1}) and for the annual mean ITCZ shift in perturbed climate states (Donohoe et al. 2013). This result suggests that the mutual dependence of P_{CENT} and AHT_{EQ} on the Hadley cell location is nearly timescale independent although the fundamental cause of the quanitative reltionship is unclear; both the intensification of the Hadley cell as the ITCZ moves off the equator and the co-location of the ITCZ with the maximum upward velocity which is equatorward of the zero streamfunction cause the ITCZ to be less sensitive to extratropical forcing than would be the case if the Hadley cell simply translated meridionally (Donohoe et al. 2013). Statistically indistinguishable statistics (i.e. correlations, regression and variance retained) between AHT_{EQ} and P_{CENT} are found using the annual-mean values (red and blue crosses in Figure 1a and thick black crosses in Figure 1b)[2]. For the remainder of this study, we will consider statistics derived from the annual-mean data when discussing the inter-annual variability. We note that the annual-mean P_{CENT} and AHT_{EQ} anomalies have standard deviations that are 44% and 55% of their monthly anomalies, respectively.

Applying Equation 1, the inter-annual variability in AHT_{EQ} is primarily (72%) due to anomalies in the MOC of the atmosphere (i.e., the Hadley Cell). The inter-annual variability of AHT_{EQ} associated with the stationary eddies and transient eddies are both approximately one order of magnitude smaller than the AHT_{EQ} variability associated with the MOC[3]. The precipitation anomaly associated with a 1° northward ITCZ shift shows an intensification of the climatological precipitation maximum in the Tropical Pacific, north of the equator, and decreases in precipitation on and south of the equator in the Pacific (Figure 2). The streamfunction anomaly associated with a 1° northward ITCZ shift (Figure 3b) shows an intensified

[2]This result suggests that the box car window filter of the annual mean does not adversely alias the time series of AHT_{EQ} and P_{CENT}; aliasing would be most problematic if there was significant variability at periods of 8 and 4 months.

[3]The dominance of the MOC in the inter-annual variability of atmospheric energy transport is in contrast to the annual mean climatology, where the MOC, stationary eddies and transient eddies all make comparable contributions to AHT_{EQ} (Marshall et al. 2013).

counter-clockwise rotating cross equatorial cell providing an anomalous energy transport (of 0.34 PW)[4] from the NH to the SH, primarily in the thermally direct streamfunction anomaly (0.24 PW is associated with the Hadley Cell anomaly and the remainder is due to stationary eddies). The precipitation anomalies show enhanced precipitation in the region of anomalous upward motion in the Hadley cell and decreased precipitation in the region of enhanced subsidence. These results collectively suggest that the inter-annual variability of the ITCZ location and the atmospheric heat transport across the equator are primarily controlled by their mutual dependence on the Hadley cell. The inter-annual variability of the Hadley cell, tropical precipitation and AHT_{EQ} is best described as an intensification of the hemispherically asymmetric features including the intensification of the precipitation maximum, cross-equatorial Hadley cell and heat transport in the thermally direct MOC.

This observed inter-annual relationship between AHT_{EQ} and ITCZ location (P_{CENT}) can be compared to that in the climatological mean (Frierson et al. 2013; Marshall et al. 2013), wherein the ITCZ location, in the NH, is accompanied by a southward AHT_{EQ} of order -0.2 PW (Figure 3a). This value of AHT_{EQ} is a consequence of (i) ocean heat transport (of about 0.4 PW) northward across the equator, and (ii) climatological radiative fluxes at the TOA that are nearly hemispherically symmetric in the shortwave (Voigt et al. 2013b) but slightly asymmetric in the longwave (cooling the NH by 0.2 PW); combined, this results in the atmosphere being heated more strongly in the NH than in the SH, setting the climatological annual-mean ITCZ position. The observed anomalies in AHT_{EQ} and ITCZ location

[4] We note that the 0.34 PW AHT_{EQ} anomaly associated with a 1° ITCZ shift is *not* equal to the reciprical of the the regression coefficeint between P_{CENT} and AHT_{EQ} of 1.6° PW^{-1} because the variables are not perfectly correlated.

on inter-annual timescales (Figure 3b) must similarly be associated with inter-hemispheric asymmetries in energy input to the atmosphere, through inter-hemispheric differences in radiative fluxes at the TOA or through surface heat flux anomalies due to ocean heat transport and storage. Distinguishing the physical processes responsible for the inter-annual variability of the hemispheric atmospheric energy budget is an unresolved issue in climate dynamics. The observational record does not allow an accurate attribution of the AHT_{EQ} anomalies to anomalies in surface fluxes (ocean heat transport and storage) and radiative anomalies at the TOA due to the sparseness and lack on temporal continuity of the direct observations of the TOA radiative fluxes and surface energy fluxes; observational estimates of the TOA radiation (CERES EBAF – Loeb et al. 2009) are only available for the 2001-2012 time period which is insufficient to provide robust correlations between ITCZ location and energy fluxes (see conclusion section for additional discussion). Thus, we turn to model simulations to ask what drives and determines the magnitude of the inter-annual variability of AHT_{EQ} and ITCZ location.

3. Coupled climate model

Thus far we have demonstrated that the inter-annual variations in ITCZ location (P_{CENT}) are strongly negatively correlated with those in atmospheric energy transport across the equator (AHT_{EQ}) over the observational record. Here, we show that the inter-annual variability of P_{CENT} and AHT_{EQ} in a coupled climate model has similar negative correlations to those found in the observations. We then attribute the inter-annual variability of AHT_{EQ} to anomalies in TOA radiation and surface fluxes related to ocean heat content changes and ocean heat transport anomalies.

We analyze a pre-industrial simulation performed with the GFDL CM2.1 coupled model (Delworth et al. 2006). The atmospheric model features a finite volume dynamical core (Lin 2004) with a horizontal resolution of approximately 2° latitude and 24 vertical levels. The ocean model is on a tripolar grid at a nominal resolution of 1° (Griffies et al. 2005). The simulation is run for 500 years with greenhouse gas and aerosol concentrations fixed at pre-industrial levels, and we perform our analysis over the last 450 years.

a. Inter-annual variability of ITCZ location and AHT_{EQ}

The annual mean anomalies of P_{CENT} and AHT_{EQ} are strongly negatively correlated (R=-0.76) with a regression coefficient of 3° PW^{-1} (thick crosses in Figure 4). Similar (statistically indistinguishable) results are found when considering the low pass filtered time series using a double pass Butterworth filter with a cutoff period of two years (solid lines in Figure 4a). The monthly variability of both P_{CENT} and AHT_{EQ} is large relative to the inter-annual variability; less than 20% of the variability is at periods more than 1 year. However, the monthly variations in P_{CENT} and AHT_{EQ} are weakly correlated (R=-0.39; thin gray crosses in Figure 4b) compared to the inter-annual variability. Therefore, we will define the inter-annual variability of P_{CENT} and AHT_{EQ} as the variance in the annual means, consistent with our analysis of the observations. We note that the correlation between AHT_{EQ} and P_{CENT} is larger in magnitude (R=-0.88) at the decadal frequency compared to inter-annual frequency, but that the variance in each is five times smaller at the decadal frequency.

The inter-annual variability of P_{CENT} in the GFDL model is primarily associated with a pulsing of the climatological precipitation maximum just north of the equator in the Pacific (not shown). The precipitation anomaly associated with a northward P_{CENT} anomaly also features a northward shift of precipitation maximum in the Indian ocean and a very weak signal in the Atlantic basin. Overall, the inter-annual variability of P_{CENT} shows a very similar spatial footprint to that found in the observations (Figure 2). The inter-annual variability of AHT_{EQ} is associated with a pulsing of the climatological annual mean Hadley cell with a southward AHT_{EQ} anomaly corresponding to an intensification of the counter-clockwise rotating cell at the equator (not shown). These results suggest that the inter-annual variability of P_{CENT} and AHT_{EQ} in the GFDL model reflect the same mutual connection between atmospheric heat transport, tropical precipitation and Hadley cell dynamics as were identified in the observational record (Figure 3).

b. Energy fluxes contributing to the inter-annual variability of AHT_{EQ}

The previous section demonstrated that the inter-annual variability of the tropical precipitation in the GFDL CM2.1 model is associated with anomalous atmospheric energy transport between the two hemispheres. The latter inter-hemispheric energy flow in the atmosphere must be balanced by an inter-hemispheric contrast in atmospheric heating either by the radiative fluxes at the TOA or by the surface energy fluxes. More formally, AHT_{EQ} can be expressed as the hemispheric asymmetry of energy fluxes to the atmosphere (and energy storage in the atmospheric column):

$$AHT_{EQ} = \langle NET_{RAD,TOA} \rangle + \langle SHF \rangle - \langle STOR_{atmos} \rangle \quad , \tag{2}$$

where $\langle\ \rangle$ brackets denote the difference between (spatially-integrated) SH-mean and global-mean values. All fluxes are defined as positive when energy is fluxed to the atmosphere; AHT_{EQ} is positive when heat is transported northward across the equator, corresponding to a stronger heating of the SH than the NH. $\langle NET_{RAD,TOA}\rangle$ is the net radiative heating of the SH at the TOA (minus the global mean radiative imbalance) which is equivalent to the net radiative cooling of the NH. $\langle SHF\rangle$ is the net heating of the SH by upward energy fluxes (turbulent and radiative) from the surface to the atmosphere. $\langle SHF\rangle$ includes the combined effects of ocean energy transport and energy storage in the ocean. In equilibrium (i.e., no ocean energy storage), $\langle SHF\rangle$ is equal (but of opposite sign) to the northward ocean heat transport across the equator ($\equiv \mathrm{OHT}_{EQ}$): southward OHT_{EQ} must be balanced by an export of energy from the atmosphere to the surface in the NH and an import of energy to the atmosphere from the ocean in SH. On the inter-annual timescale, the hemispheric asymmetry of oceanic energy storage contributes to $\langle SHF\rangle$ with preferential oceanic energy storage in the NH corresponding to a positive $\langle SHF\rangle$ because the atmosphere must export energy to the ocean in the NH. $\langle STOR_{atmos}\rangle$ is the hemispheric asymmetry of the atmospheric column integrated energy (sensible plus latent) tendency and is positive when the temperature or humidity of the atmosphere is increasing in the SH which serves as a pseudo sink of energy in the SH (note the negative sign in Equation 2) .

Time series of AHT_{EQ} and its decomposition into the hemispheric asymmetry of energy fluxes to the atmosphere via Equation 2 are shown in Figure 5. The inter-annual variability of AHT_{EQ} has a standard deviation of $\sigma = 0.08$ PW. The inter-annual variability of $\langle NET_{RAD,TOA}\rangle$ ($\sigma = 0.073$ PW) is slightly larger but comparable in magnitude to that of $\langle SHF\rangle$ ($\sigma = 0.058$ PW). The inter-annual variability of atmospheric energy storage

($\langle STOR_{atmos} \rangle$) makes a smaller contribution to inter-annual variability of the hemispheric energy budget ($\sigma = 0.017$ PW) than the TOA and surface energy fluxes. Over the 450 year simulation (see Figure 5), anomalies in AHT$_{EQ}$ (black lines) are most strongly correlated with anomalies in $\langle NET_{RAD,TOA} \rangle$ (R = 0.67 – red lines) and are less strongly correlated with anomalies in $\langle SHF \rangle$ (R = 0.30 – blue lines). The lead and lag relationships between P$_{CENT}$, AHT$_{EQ}$, $\langle NET_{RAD,TOA} \rangle$ and $\langle SHF \rangle$ are calculated from the low pass filtered time series using a cutoff period of two years. On average, P$_{CENT}$ anomalies lead AHT$_{EQ}$ of the opposite sign by three months as deduced from the time lag of optimal negative correlation. The hemispheric asymmetry of net radiation at the TOA ($\langle NET_{RAD,TOA} \rangle$) is in phase with P$_{CENT}$ and leads the AHT$_{EQ}$; optimal lagged correlations occur for $\langle NET_{RAD,TOA} \rangle$ leading AHT$_{EQ}$ by three months with a correlation of 0.69. In contrast, the hemispheric asymmetry of surface energy fluxes ($\langle SHF \rangle$) lag the AHT$_{EQ}$ on average; optimal lagged correlations occur for $\langle SHF \rangle$ lagging AHT$_{EQ}$ by three months with a correlation of 0.49. The lead lag relationships discussed above are qualitatively over all 100 year subsets of the simulation. Collectively, these results suggests that the inter-annual variability of AHT$_{EQ}$ and, thus, the ITCZ location, is primarily a consequence of inter-annual variations in radiation at the TOA in the GFDL model although it is unclear if the radiation anomaly is itself a manifestation of the ITCZ shift or forces the ITCZ shift.

We now ask: what regions contribute to the hemispheric asymmetries in energy fluxes for a "typical" P$_{CENT}$ anomaly? Figure 6 shows the regression of the inter-annual variability of AHT$_{EQ}$ onto the anomalies of the net radiative flux at the TOA (left panel) and surface fluxes (right panel) normalized to a -0.34 PW AHT$_{EQ}$ anomaly, which corresponds to a 1° northward ITCZ shift. The energy fluxes are defined as positive when energy flows into the atmosphere. The TOA radiative flux associated with the southward AHT_{EQ} anomaly is positive in the Tropical Pacific just north of the equator where the precipitation and cloud cover have increased concurrently with the northward shift of the ITCZ (the increased precipitation is indicated with the purple contours). In this region, the enhanced cloud cover results in less absorbed shortwave radiation (more reflection off the clouds) and reduced emitted longwave radiation as the OLR is emitted from higher in the atmospheric column where temperatures are colder (not shown). The magnitude of the reduced OLR (an energy gain) is larger than that of the reduced absorbed shortwave radiation (energy loss). Thus, shifting the ITCZ to the north results in atmospheric heating in the NH and cooling in the SH due to the net radiative cloud response. This mechanism acts as a positive feedback on ITCZ migration as the enhanced heating in the hemisphere to which the ITCZ has shifted requires that additional energy be fluxed to the other hemisphere, which is most readily accomplished by shifting the Hadley cell in the same sense of the initial perturbation. Thus, the local TOA radiation change associated with an ITCZ shift demands a cross equatorial atmospheric heat transport that shifts the Hadley cell in the same direction as the initial perturbation. We note that the radiative anomalies are primarily confined to the tropics and are manifestations of the ITCZ shift itself; extratropical radiative forcing does not play a prominent role in forcing inter-annual variations in AHT_{EQ} in the GFDL model, which is a stark contrast to the role of extratropical cloud radiative forcing in the climatological response of the ITCZ to anthropogenic forcing (Frierson and Hwang 2012).

The surface heat flux anomaly associated with a northward P_{CENT} shift is also dominated by a tropical signal with anomalous energy fluxes into the ocean in the Eastern Pacific and anomalous energy fluxes to the atmosphere over a smaller region in the far Western Pacific (right panel of Figure 6). The surface heat flux anomaly that accompanies the northward ITCZ shift is more symmetric about the equator than its TOA radiation counterpart (c.f. the red and blue zonal mean in the middle panel of Figure 6). We will show in the following section that the inter-annual variability of ocean energy fluxes and storage in the deep tropics are of order 100 W m^{-2} and nearly compensating; the inter-annual variability of the upward surface heat flux is the small residual of large variations in the ocean energy transport divergence and the storage of energy within the oceanic column. As a result, the atmospheric and oceanic meridional energy transport do not compensate for one another on the inter-annual timescale because the vast majority of the ocean energy transport anomalies are stored locally in the ocean and therefore never impact the atmospheric energy budget.

c. *The role of inter-annual variability in ocean circulation on the hemispheric energy budget*

We now explore the role of inter-annual variability in the strength of the ocean circulation on the inter-annual variability of AHT_{EQ} and therefore P_{CENT}. Previous studies (Marshall et al. 2013; Frierson et al. 2013) have demonstrated that the approximately 0.7 PW of northward energy transport of the AMOC across the equator (Ganachaud and Wunsch 2003) is the cause of the annual mean position of the ITCZ north of the Equator. Previous studies have linked the multi-decadal variability of the AMOC with large scale precipitation anomalies (Zhang and Delworth 2006). Tulloch and Marshall (2013) demonstrated that the AMOC in the GFDL CM2.1 model varies inter-annually by approximately 15% of the climatological mean value (i.e. AMOC OHT_{EQ} varies by of order 0.1 PW). Yet, we did not see a manifestation of the inter-annual variability of the AMOC in the surface heat fluxes leading to an AHT_{EQ} anomaly (right panel of Figure 6). In this section, we ask why the inter-annual variability in the ocean heat transport across the equator is not accompanied by a compensating atmospheric heat transport across the equator.

We define an index of the variability of the AMOC by averaging the monthly anomaly (from climatology) of the AMOC streamfunction between 100m and 3000m and between 10°S and 10°N (the region inside the purple box in Figure 7b). A time series of the AMOC index (Figure 7a) demonstrates that the AMOC at the equator varies by approximately 2.0 Sv (1σ) from month to month which is approximately 20% of the climatological mean value of 10.6 Sv. The inter-annual variability of the AMOC index explains the majority (R=0.82) of the ocean heat transport anomalies across the equator in the Atlantic (not shown). The AMOC index has very little memory from month to month; the decorrelation timescale is less than one month. This short term variability in the AMOC is primarily due to shallow Ekman transport anomalies associated with zonal wind stress anomalies; the accompanying energy flux anomalies are nearly entirely stored locally in the ocean and never impact the atmospheric column. For this reason, we choose to focus on the lower frequency variability of the AMOC which we define using a low pass Butterworth filter with a cutoff period of 6 years (blue line in the top panel of Figure 7)[5]. Much of the low frequency variability of the AMOC in the GFDL model is at the decadal frequency (Tulloch and Marshall 2013). The low frequency AMOC index has an amplitude of approximately 25% of that in monthly data. The cross section of AMOC streamfunction anomalies associated with a 1σ low frequency AMOC index anomaly (middle panel of Figure 7) demonstrates that the low frequency AMOC anomalies are strongly correlated over the upper 3000m of the column and from

[5]Using a cutoff period of two years, as in the previous section, produces qualitativlely similar results.

20°S to 45°N with peak anomalies North of the equator.

The ocean heat transport anomalies must either be balanced by storage in the oceanic column (a change in potential temperature) or by upward surface energy fluxes to the atmosphere:

$$\nabla \cdot OHT = SHF + STOR_{OCEAN} \tag{3}$$

We calculate the energy storage in the oceanic column (STOR$_{OCEAN}$) as the tendency (centered finite difference) of the mass integral of C$_{P,ocean}\Theta$ where C$_{P,ocean}$ is the heat capacity of ocean water and Θ is the potential temperature. The surface heat flux (SHF – positive to the atmosphere) is directly outputted on the ocean grid. $\nabla \cdot OHT$ is calculated as the residual of Equation 3. The ocean heat transport anomaly is calculated as the spatial integral of $\nabla \cdot OHT$ over the polar cap poleward of each latitude.

The ocean heat transport anomaly associated with the AMOC anomaly (bottom panel of Figure 7) shows the expected northward heat transport anomaly at the equator of order 0.1 PW. We note that approximately half of this ocean heat transport anomaly is associated with the Atlantic basin with maximum ocean heat transport convergence in the mid-latitude (Figure 8B) and the remainder is due to ocean circulation changes in the Pacific where the heat transport convergence occurs in the subtropics. The approximately 0.05 PW of northward heat transport associated with the 0.5 Sv AMOC index anomaly corresponds to a potential temperature difference of 25K between the anomalous northward flow at the surface and the southward return flow at depth which is consistent with the ocean's static stability in the tropics in the model. By construction, the ocean heat transport across a given latitude circle is balanced by the sum of the spatial integrals of SHF and STOR over the polar cap north of that latitude (i.e. the black and red lines in Figure 7 sum to the blue line). By and large, the anomalous ocean heat transport associated with an AMOC index anomaly is balanced by ocean heat storage poleward of the energy flux anomaly and only secondarily by fluxes to the atmosphere. More specifically, the 0.10 PW of anomalous northward ocean heat transport at the equator goes entirely into ocean energy storage and never gets fluxed upward to the atmosphere. As a consequence, the atmospheric energy budget is unaffected by the ocean heat transport anomaly; there is no compensating atmospheric heat transport to the ocean heat transport anomaly, and thus the tropical precipitation is unaffected by the AMOC anomaly. There is no significant correlation between the AMOC index and AHT_{EQ} or P_{CENT} even when lagged correlations are considered and when AMOC anomalies at different latitudes are considered. This conclusion also holds when considering the decadal variability of the AMOC (i.e. using a 20 year period low pass filter).

The spatial maps of anomalous $\nabla \cdot OHT$ associated with a 1σ AMOC index (Figure 8) and its allocation between SHF and STOR_{ocean} show that the vast majority of the anomalous $\nabla \cdot OHT$ is in the extratropical North Atlantic. The anomalous ocean heat transport convergence in the North Atlantic is balanced by local storage as opposed to surface energy fluxes out of the ocean (c.f. the bottom left and bottom right panels of Figure 8). The SHF anomaly associated with an AMOC index anomaly are smaller in magnitude than the corresponding ocean heat storage anomaly and feature a dipole in the vicinity of the Gulf Stream. We speculate that this anomalous SHF is associated with a concurrent shift in the Gulf Stream and is not related to the ocean heat transport anomaly in the AMOC.

We now ask: why doesn't the inter-annual variability of the AMOC energy transport (of order 0.1 PW) impact the atmospheric energy budget by way of the surface energy fluxes?

The most obvious explanation is that the ocean heat transport anomalies are converged deep within the oceanic column and therefore do not impact the SSTs and surface energy fluxes. Indeed, the vertical profile of oceanic temperature tendencies associated with an AMOC index anomaly (colored field in the middle panel of Figure 7) show that, in the region of anomalous AMOC energy flux convergence, around 50°N, the heating occurs primarily below the ocean mixed layer and extends all the way down to 4 km depth. At the surface, the anomalously strong AMOC causes cooling in the vicinity of 60°N and a slight warming in the deep tropics; there is only a hint of surface warming in the northern extratropics due to the AMOC anomaly (over the limited region around 45°N). The SST anomaly associated with a one standard deviation AMOC index shows slight warming ($\approx$ 0.2 K) over a limited domain poleward of 45°N (not shown). Overall, the canonical view of AMOC anomalies influencing the extratropical climate system in the North Atlantic is unrealized in the interannual variability of the GFDL model, because the AMOC anomalies only influence ocean temperatures at depth.

4. Summary and discussion

Previous work has demonstrated that the relationship between ITCZ location and atmospheric heat transport across the equator is quantitatively consistent across a myriad of timescales ranging from the seasonal cycle to the annual mean climatology and the shift due to external forcing. The dominant physical processes contributing to the AHT_{EQ} by way of the hemispheric asymmetry of energy input into the atmosphere vary with timescale. In the annual mean climatology, the hemispheric asymmetry of atmospheric heating is dominated by the upward surface heat fluxes by way of the ocean heat transport across the equator (Marshall et al. 2013). On decadal and shorter timescales, the anomalies in the ocean heat transport and radiative energy input into the surface are stored within the ocean column and, thus, do not contribute to the atmospheric energy budget. Indeed, over the seasonal cycle, variations in AHT_{EQ} are driven by the absorption of insolation in the atmospheric column (Donohoe et al. 2013) and opposed by the surface fluxes as the ocean energy storage in the summer hemisphere exceeds the input of energy into the surface by radiative process and ocean heat transport convergence (Donohoe and Battisti 2013). Here, we focus on an intermediate timesacale; the inter-annual (2-10 year) variability.

We demonstrate that the inter-annual variability of ITCZ location and AHT_{EQ} are strongly (negatively) correlated in Nature (R=-0.75) and a coupled climate model (R=-0.76). A 1° northward ITCZ shift is associated with approximately -0.33 PW of southward AHT_{EQ} which is statistically indistinguishable from the relationship found over the seasonal cycle and the annual mean response due to external climate forcing (Donohoe et al. 2013). The inter-annual variability of AHT_{EQ} and ITCZ location both reflect a mutual connection to an intensification of the climatological Hadley cell and the concurrent intensification of the climatological precipitation maximum (Figure 3). The cause of the inter-annual variability on AHT_{EQ} by way of the hemispheric scale atmospheric energy budget is diagnosed in the climate model (such analysis is not possible in the observations). The inter-annual variability of AHT_{EQ} is primarily due to hemispheric asymmetries in radiative fluxes at the TOA, secondarily due to surface energy fluxes and has a weak dependence on atmospheric energy storage (Figure 5). The radiative flux anomalies associated with a northward ITCZ shift are primarily a consequence of the ITCZ shift itself with more intense deep convection

North of equator resulting in a net radiative heating anomaly in the NH (Figure 6). The increased convection north of the equator causes reduced OLR as radiation is emitted from higher in the atmospheric column (due to both water vapor and cloud feedbacks) where air is colder. The absorbed shortwave radiation also decreases north of the equator due to increased cloud reflection. In the net, the OLR feedback is stronger in magnitude. As a result, a northward shifted ITCZ results in stronger atmospheric heating in the NH which serves as a positive feedback for ITCZ migration; the Hadley cell shift required to achieve the AHT_{EQ} demanded by the global scale TOA radiative budget shifts the ITCZ in the same sense as the initial perturbation. We note that this conclusion may be model dependent (Voigt et al. 2013a) and we have only demonstrated the net positive radiative feedback in the GFDL CM2.1 model.

A determination of the energetic source of inter-annual variability of AHT_{EQ} in Nature is limited by our observations of the both the TOA radiation and the surface energy fluxes; the observed atmospheric energy budget is not closed on the inter-annual timescale. In the global mean climatology, the TOA energy budget is not closed to within 5 W m^{-2} (Loeb et al. 2009). How these observational uncertainties project onto hemispheric asymmetries of energy input to the atmosphere at the inter-annual timescale is unclear. TOA radiative anomalies from CERES EBAF are available for the 2001-2012 time period and could provide insights about whether the processes responsible for the inter-annual variability of AHT_{EQ} in the GFDL model are also realized in the observations. Preliminary work suggests that radiative feedbacks explain a significant portion of the inter-annual variability of AHT_{EQ} and that the ITCZ shift induces a positive radiative feedback on the atmospheric heating (warming the hemisphere that the ITCZ has shifted toward).

Why doesn't the inter-annual variability of ocean heat transport have an impact on ITCZ location? Indeed, the inter-annual variability of the AMOC ocean heat transport across the equator (≈ 0.1 PW) is comparable in magnitude to the inter-annual variability of AHT_{EQ} ($\sigma = 0.08$ PW) in the GFDL CM2.1 model. However, the latter is not influenced by the former. The reason the AMOC (and the ocean heat transport across the equator in general) does not influence the atmosphere on the inter-annual timescale is that the vast majority of AMOC heat transport anomalies are stored within the ocean, below the surface (Figure 7) and, thus, do not enter the atmospheric column (lower right panel of Figure 8). Similar results are found when considering the decadal variability of the AMOC which has been shown to be significant and predictable in this model (Tulloch and Marshall 2013). This result suggests that the inter-annual variability of ocean circulation plays a negligible role in the inter-annual variability of atmospheric energy fluxes because the latter is dominated by TOA radiative fluxes which are very sensitive to even modest changes in clouds.

The impact of ocean heat transport on the atmospheric circulation varies drastically with timescale (Figure 9). On short timescales (years to decades), energy is stored in the oceanic column, has a small expression on SSTs and very little energy gets fluxed upward to the atmosphere to impact the atmospheric circulation (the red– storage– lines have larger magnitudes than the blue – surface flux– lines on the high frequency side of Figure 9). On very long timescales (climatology), the surface energy budget requires that the entirety of the ocean heat transport convergence be fluxed upward to the atmosphere and is thus the dominant mechanism of the hemispheric contrast of energy input to the atmosphere. At what timescale, then, does the ocean heat transport impact the hemispheric scale atmospheric energy budget and thus the ITCZ position? In the GFDL CM2.1 model, half of the OHT_{EQ}

is fluxed upward to the atmosphere at a timescale of 35 years in the Atlantic (where the dashed red and blue line cross in Figure 9) whereas the same timescale is longer in the other ocean basins. This result suggests that the AMOC may impact the atmospheric energy budget and, thus, the ITCZ at the multi-decadal frequency as was found by Zhang and Delworth (2006).

The positive feedback between ITCZ shifts and AHT_{EQ} induced by the tropical cloud feedbacks in the GFDL model relies on the positive longwave cloud feedback associated an increase in convective clouds in the tropics being larger in magnitude than the negative shortwave cloud feedback. It is unclear if this relationship is robust across different models and is evident in Nature. Recent work by Voigt et al. (2013a) suggests that tropical radiative feedbacks play a negligible role in determining the magnitude of the ITCZ shift in response to hemispheric scale forcing in the ECHAM6 model whereas Kang et al. (2008) previously found that cloud radiative feedbacks provide a negative feedback to ITCZ shifts. Preliminary analysis of the inter-annual variability of observations (CERES EBAF – Loeb et al. 2009) suggests that radiative anomalies provide a small net tropical heating anomaly (≈ 1 W m^{-2}) to the hemisphere to which the ITCZ has shifted (not shown). In the GFDL model, tropical radiation anomalies (equatorward of 20°) associated with anomalous southward AHT_{EQ} (Figure 6) account for approximately half (45%) of the hemispheric asymmetry of energy input to the atmosphere demanded by the AHT_{EQ} anomaly. If we assume that the magnitude of tropical radiation anomalies is proportional to the AHT_{EQ} (i.e. the magnitude of the ITCZ shift) this result suggests that tropical cloud feedbacks amplify the ITCZ shift due to external forcing by a factor of two; the ITCZ shift required to export a given energy input into the NH is twice as large when tropical radiative feedbacks are active as compared to a system with no tropical radiaitive feedbacks. More formally, the feedback gain of tropical radiative feedbacks can be shown to be approximately two relative to a reference system with no tropical cloud feedbacks. We note that this result is at odds with the work of Voigt et al. (2013a) that found little amplification of ITCZ shifts by radiative feedbacks in ECHAM6.

An alternative negative feedback to an ITCZ perturbation is that the wind driven components of the oceanic and atmospheric energy transport are coupled via the surface wind stress (and Ekman dynamics) and transport energy in the same direction (Held 2001) in both the climatology and the anomalous sense. Therefore, if the system is externally forced by a hemispheric asymmetry of atmospheric heating, the anomalous AHT_{EQ} and OHT_{EQ} will be in the same direction with each fluid carrying comparable quantities of energy. On short timescales, the ocean heat transport anomaly is stored within the ocean and the atmospheric energy budget is unaffected. On longer timescales, as the ocean heat storage decreases, the OHT_{EQ} anomaly is fluxed upward to the atmosphere and the hemispheric asymmetry of surface heat fluxes opposes the initial external forcing. In equilibrium, the inter-hemispheric energy flow demanded by the external forcing is achieved by the sum of the AHT_{EQ} and the OHT_{EQ} which are in the same direction and comparable in magnitude. Therefore, the AHT_{EQ} anomaly in an externally forced coupled (interactive ocean) system is significantly smaller than it is in the uncoupled system (atmosphere only). This mechanism is expected to decrease the sensitivity of ITCZ migration to external forcing that has been deduced from atmospheric only simulations (i.e Yoshimori and Broccoli 2008; Kang et al. 2008).

We note that, the inter-annual variability of P_{CENT} is also significantly correlated with the inter-hemispheric difference in tropical SSTs – defined as the difference between the spatially averaged SST between the equator and 20°N and that between the equator and

20°S (Donohoe et al. 2013)– in Nature (R=0.61) and in the coupled climate model (R=0.69). This suggests that the ITCZ location, the atmospheric heat transport across the equator, and the tropical SSTs all adjust in concert such that the ITCZ is located in the warmer hemisphere where the atmosphere is heated more strongly. Though this relationship is self-consistent, there is an issue of causality: is the ITCZ location dictated by the SSTs or the hemispheric scale energy budget? This work has focused on the connection between the hemispheric scale energy budget and ITCZ location in an attempt to dissect the relative roles of radiation and surface heat fluxes in determining the inter-annual variability of AHT_{EQ} and thus ITCZ location. While we find that radiative processes at the TOA play a more prominent role than surface fluxes in the hemispheric scale energy budget at the inter-annual timescale, this conclusion is likely timescale dependent. At short timescales, the ocean heat transport and SSTs/surface energy fluxes are decoupled due to ocean energy storage while at longer timescales the ocean heat transport gives rise to SST anomalies and surface fluxes. Indeed, preliminary work indicates that at the multi-decadal timescale the ITCZ location is well correlated with persistent SST anomalies which result from decadal variability in the ocean heat transport.

Acknowledgments.

We thank Aiko Voigt and three anonymous reviewers for insightful comments and suggestions. AD was supported by the NOAA Global Change Postdoctoral Fellowship. KA was funded by the James S. McDonnell Foundation Postdoctoral Fellowship.

REFERENCES

Chiang, J. and C. Bitz, 2005: The influence of high latitude ice on the position of the marine intertropical convergence zone. *Climate Dyn.*, DOI 10.1007/s00 382–005–0040–5.

Delworth, T. L., A. J. Broccoli, A. Rosati, R. J. Stouffer, V. Balaji, J. A. Beesley, and W. F. Cooke, 2006: GFDL's CM2 global coupled climate models. part i: Formulation and simulation characteristics. *J. Climate*, **19 (5)**, 643–674.

Donohoe, A. and D. Battisti, 2013: The seasonal cycle of atmospheric heating and temperature. *J. Climate*, **26 (14)**, 4962–4980.

Donohoe, A., J. Marshall, D. Ferreira, and D. McGee, 2013: The relationship between itcz location and atmospheric heat transport across the equator: from the seasonal cycle to the last glacial maximum. *J. Climate*, **26 (11)**, 3597–3618.

Frierson, D., et al., 2013: Why does tropical rainfall peak in the northern hemisphere? the role of the oceans meridional overturning circulation. *Nature Geosci.*, **6**, 940–944.

Frierson, D. M. W. and Y.-T. Hwang, 2012: Extratropical influence on itcz shifts in slab ocean simulations of global warming. *J. Climate*, **25**, 720–733.

Ganachaud, A. and C. Wunsch, 2003: Large-scale ocean heat and freshwater transports during the world ocean circulation experiment. *J. Climate*, **16**, 696–705.

Griffies, S., et al., 2005: Formulation of an ocean model for global climate simulations. *Ocean Sciences*, **1**, 45–79.

Hadley, G., 1735: Concerning the cause of the general tradewinds. *Philos. Trans. Roy. Soc*, **29**, 58–62.

Held, I., 2001: The partitioning of the poleward energy transport between the tropical ocean and atmosphere. *J. Atmos. Sci.*, **58**, 943–948.

Kalnay, E., et al., 1996: The NCEP/NCAR 40-year reanalysis project. *Bull. Amer. Meteor. Soc.*

Kang, S., I. Held, D. Frierson, and M. Zhao, 2008: The response of the itcz to extratropical thermal forcing: idealized slab-ocean experiments with a gcm. *J. Climate*, **21**, 3521–3532.

Lin, S. J., 2004: A ”vertically lagrangian” finite-volume dynamical core for global models. *Mon. Weath. Rev.*, **132 (10)**, 2293–2307.

Loeb, N. G., B. A. Wielicki, D. R. Doelling, G. L. Smith, D. F. Keyes, S. Kato, N. Manalo-Smith, and T. Wong, 2009: Towards optimal closure of the earth’s top-of-atmosphere radiation budget. *J. Climate*, **22**, 748–766.

Lorenz, E., 1953: A multiple index notation for describing atmospheric transport processes.

Marshall, J., A. Donohoe, D. Ferreira, and D. McGee, 2013: The oceans role in setting the mean position of the inter-tropical convergence zone. *Climate Dyn.*, 14.

Priestley, C., 1948: Heat transport and zonal stress between latitudes. *Quart. J. Roy. Meteor. Soc.*, **75**, doi:28-40.

Trenberth, K. E., 1997: Using atmospheric budgets as a constraint on surface fluxes. *J. Climate*, **10**, 2796–2809.

Trenberth, K. E. and J. M. Caron, 2001: The atmospheric energy budget and implications for surface fluxes and ocean heat transports. *Climate Dyn.*, **17**, 259–276.

Tulloch, R. and J. Marshall, 2013: Exploring mechanisms of variability and predictability of atlantic meridional overturning circulation in two coupled climate models. *J. Climate*, In press.

Voigt, A., B. Stevens, J. Bader, and T. Mauritsen, 2013a: Compensation of hemispheric albedo asymmetries by shifts of the itcz and tropical clouds. *J. Climate*, In press.

Voigt, A., B. Stevens, J. Bader, and T. Mauritsen, 2013b: The observed hemispheric symmetry in reflected shortwave irradiance. *J. Climate*, **26**, 468–477.

Xie, P. and P. Arkin, 1996: Analyses of global monthly precipitation using gauge observations, satellite estimates, and numerical model predictions. *J. Climate*, **9**, 840–858.

Yoshimori, M. and A. J. Broccoli, 2008: Equilibrium response of an atmospheremixed layer ocean model to different radiative forcing agents: Global and zonal mean response. *J. Climate*, **21**, 4399–4423.

Yoshimori, M. and A. J. Broccoli, 2009: On the link between hadley circulation changes and radiative feedback processes. *Geophys. Res. Lett.*, **36**, doi:10.1029/2009GL040 488.

Zhang, R. and T. Delworth, 2005: Simulated tropical response to a substantial weakening of the atlantic thermohaline circulation. *J. Climate*, **18 (12)**, DOI: 10.1029/2006GL026 267.

Zhang, R. and T. Delworth, 2006: Impact of atlantic multidecadal oscillations on India/Sahel rainfall and atlantic hurricanes. *J. Geophys. Res.*, **33 (L17712)**, DOI: 10.1029/2006GL026 267.

List of Figures

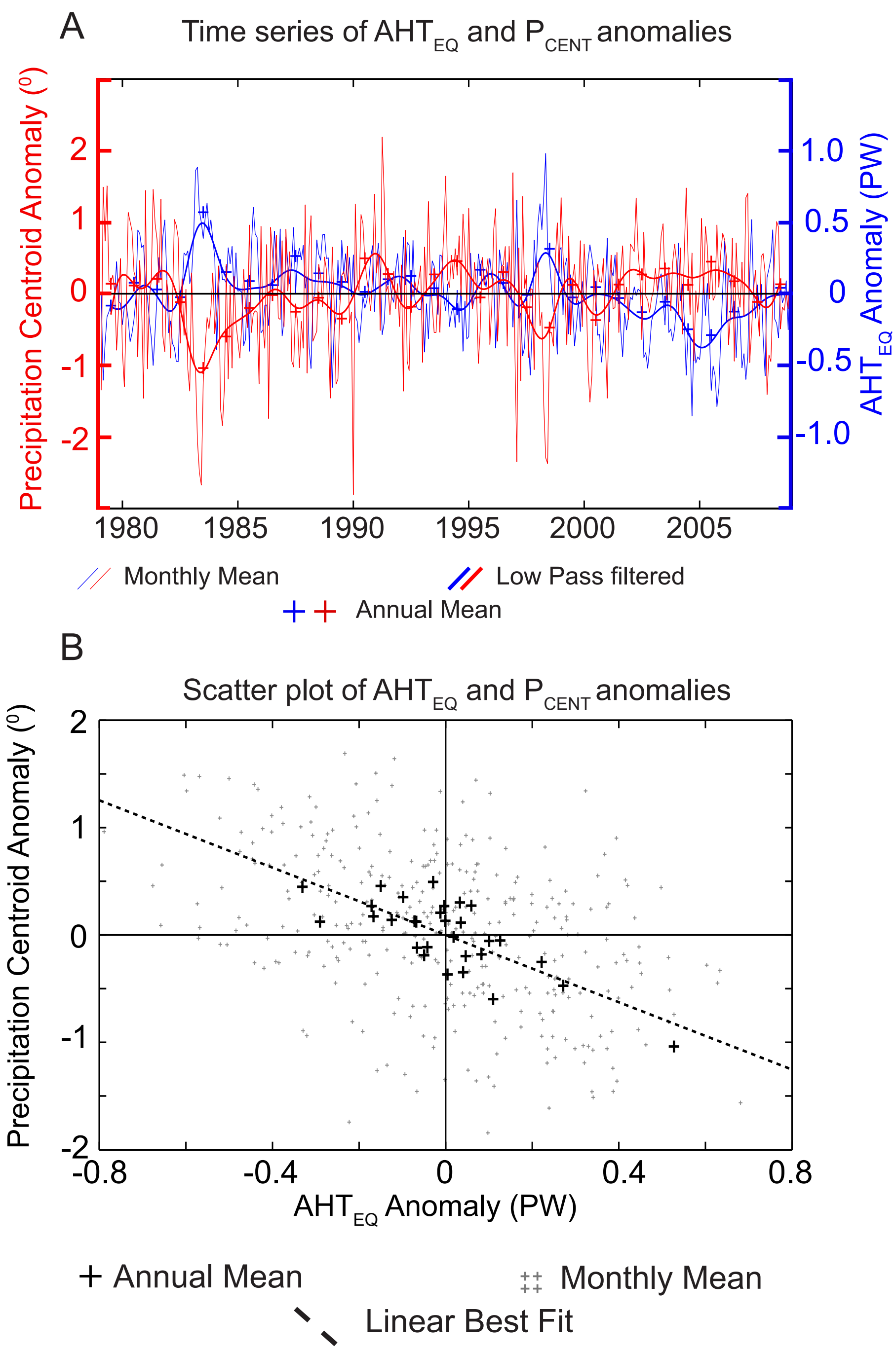

FIG. 1. (A) Time series of ITCZ location anomaly as measured by the P_{CENT} (red) and the anomaly in atmospheric heat transport at the equator (blue). The thin lines are the monthly mean anomalies and the thick lines are the low pass filtered time series (cutoff period of 2 years). The thick crosses are the annual mean anomalies from the climatology. (B) Scatter plot of the anomalies in P_{CENT} and AHT_{EQ}. The small gray crosses are the monthly means and the thick black crosses are the annual means. The dashed black line is the linear best fit to the annual mean data.

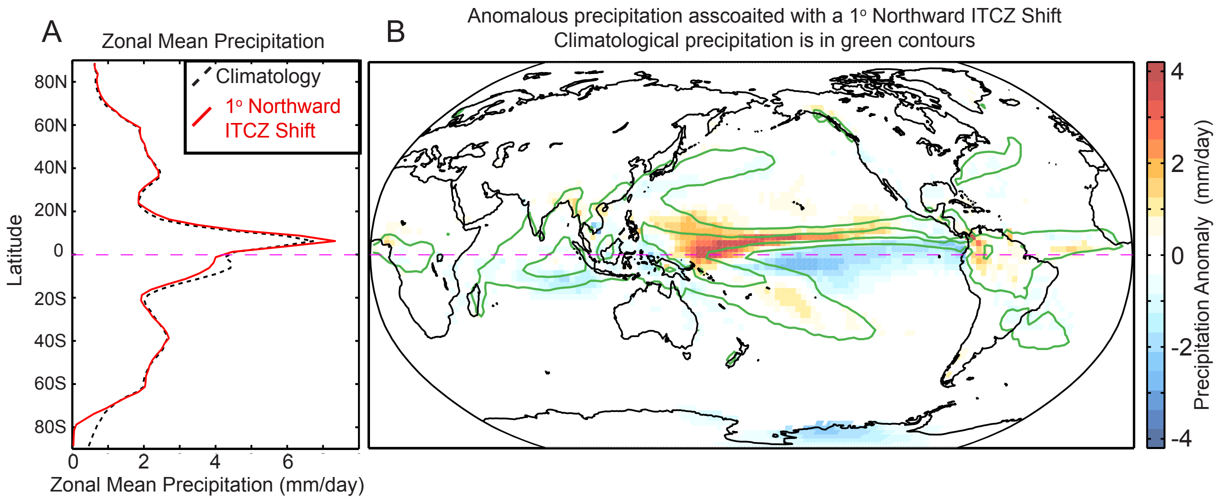

Fig. 2. (A) Zonal mean precipitation climatology (dashed black line) and precipitation associated with a 1° Northward shift in ITCZ location (red) calculated from regressing the annual mean P_{CENT} anomaly onto the annual and zonal mean precipitation anomaly. (B) Map of precipitation anomaly associated with a 1° Northward shift in zonal mean P_{CENT} evaluated from the inter-annual variability. The green contours are the climatological precipitation with a contour interval of 4 mm/day (zero contour omitted). The dashed purple line is the equator.

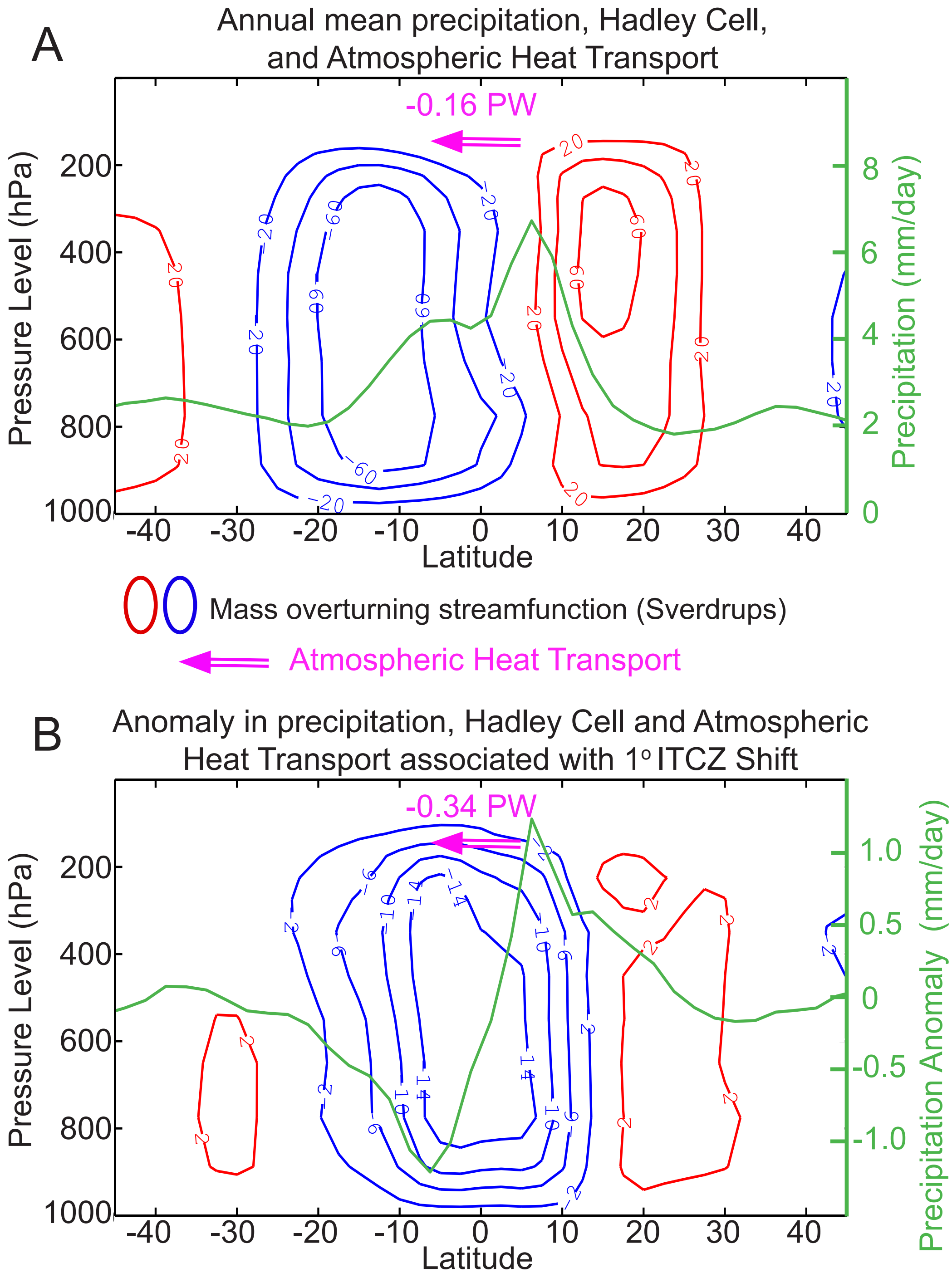

FIG. 3. (Top panel) Climatological annual mean stream function (contours) in Sv (1Sv = $10^9 kgs^{-1}$) co-plotted with the zonal mean precipitation (green- scale on the right axis). The AHT_{EQ} is indictaed in the pink arrow. (Bottom panel) As in the top panel except for the annual mean anomalies associated with a 1° Northward ITCZ shift calculated from regression of inter-annual varaibility of P_{CENT} onto the streamfunction and precipitation.

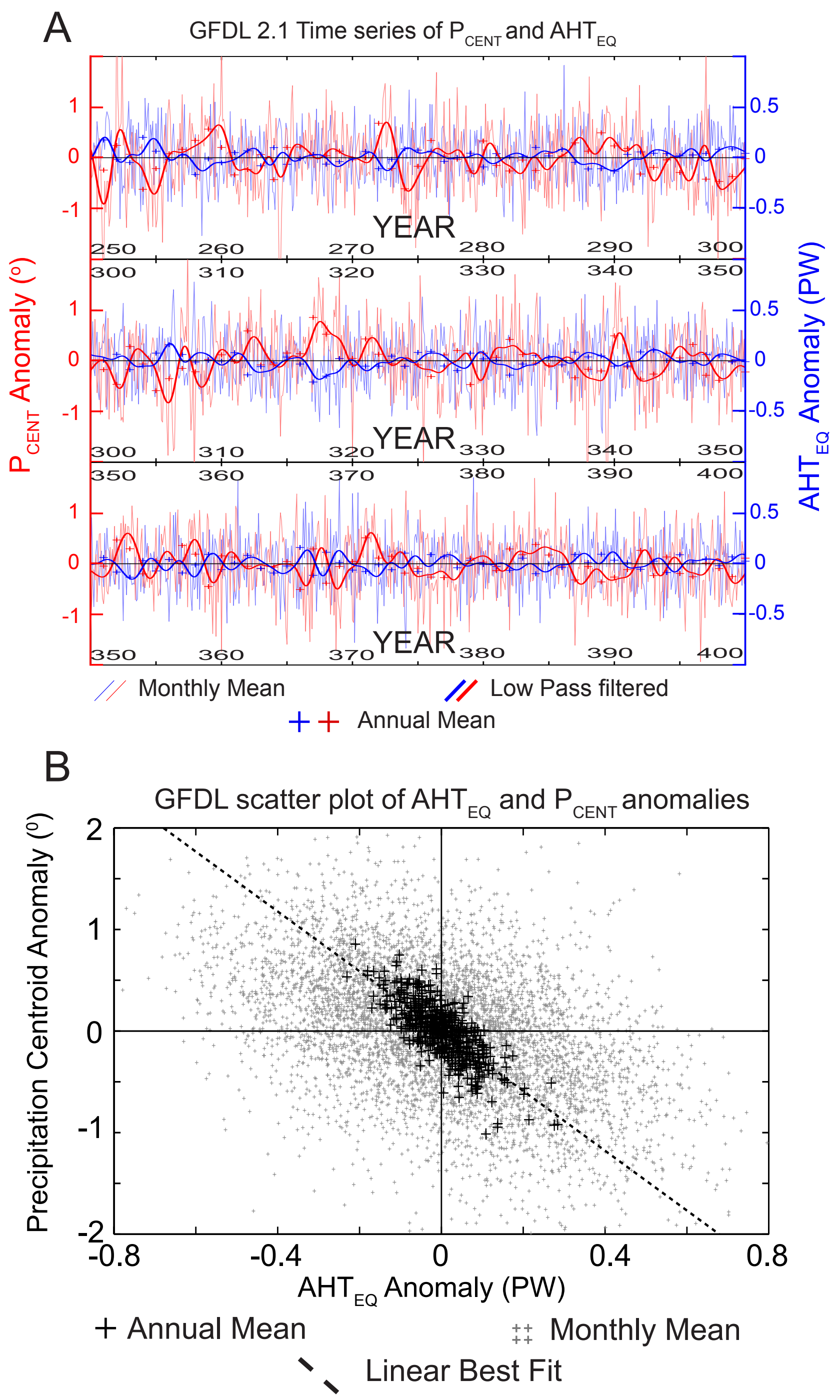

FIG. 4. (A) Time series of ITCZ location anomaly – as measured by the P_{CENT} (blue)– and the anomaly in atmospheric heat transport at the equator (red) in the GFDL 2.1 pre-industrial simulation. The thin lines are the monthly mean anomalies and the thick lines are the low pass filtered time series (cutoff period of 2 years). The thick crosses are the annual mean anomalies from the climatology. Only years 250-400 of the 500 year simylation are shown. (B) Scatter plot of the anomalies in P_{CENT} and AHT_{EQ}. The small gray crosses are the monthly means and the thick black crosses are the annual means. The dashed black line is the linear best fit to the annual mean data.

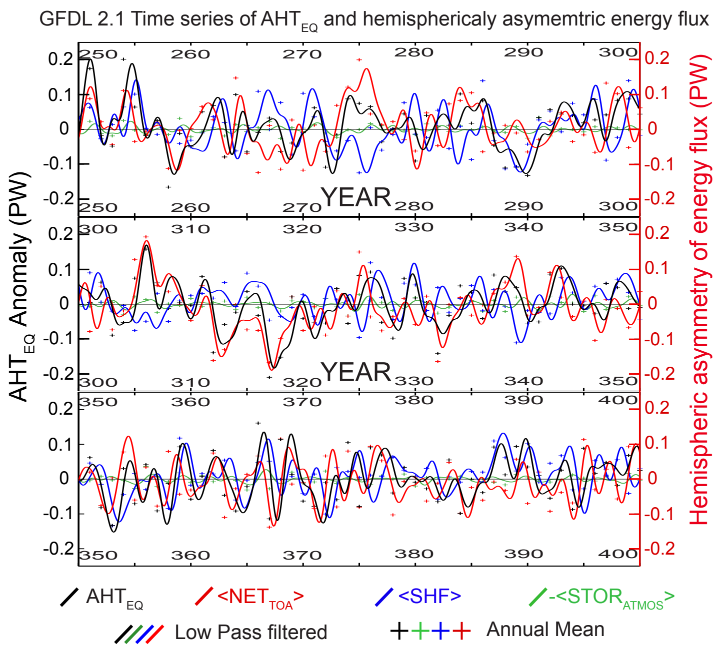

FIG. 5. Time series of the AHT$_{EQ}$ in the GFDL 2.1 pre-industrial simulation and its decomposition into the hemispheric asymmetry of TOA radiation ($\langle NET_{RAD,TOA}\rangle$ – red), surface energy fluxes ($\langle SHF\rangle$ – blue) and storage in the atmospheric column ($\langle STOR_{atmos}\rangle$ – green) from Equation 2. The thick lines are the low pass filtered time series (cutoff period of 2 years). The thick crosses are the annual mean anomalies from the climatology. Only years 250-400 of the 500 year simulation are shown.

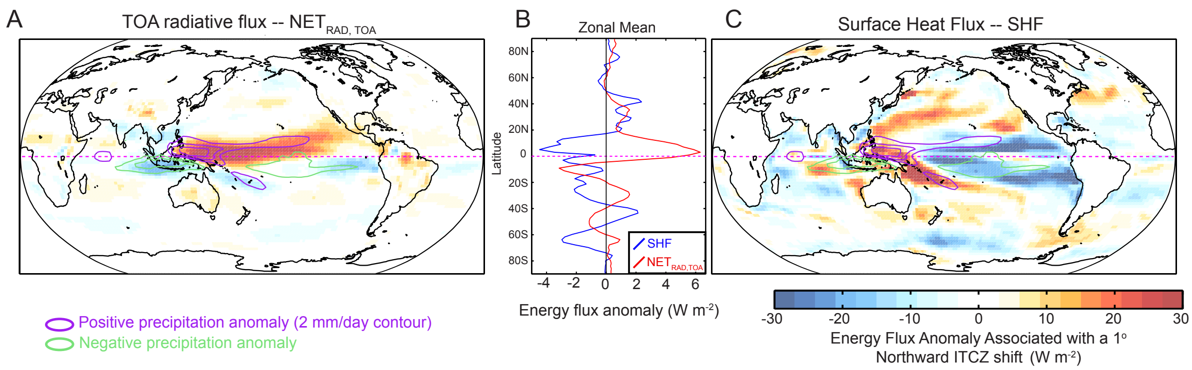

FIG. 6. Regression maps of TOA radiative anomaly (A) and surface heat flux anomaly (C) associated with a -0.34 PW AHT_{EQ} annual mean anomaly which is the AHT_{EQ} associated with a 1° northward ITCZ shift in the GFDL pre-industrial simulation. The energy fluxes are defined as positive when energy flows into the atmosphere (positive downward at the TOA and positive upward at the surface). The contours are the associated precipitation anomaly (contour interval 2 mm/ day) with green contours indicating a decrease in precipitation and purple contours indicating an increase in precipitation. (B) Zonal mean anomalies of the TOA radiative fluxes (red) and surface fluxes (blue).

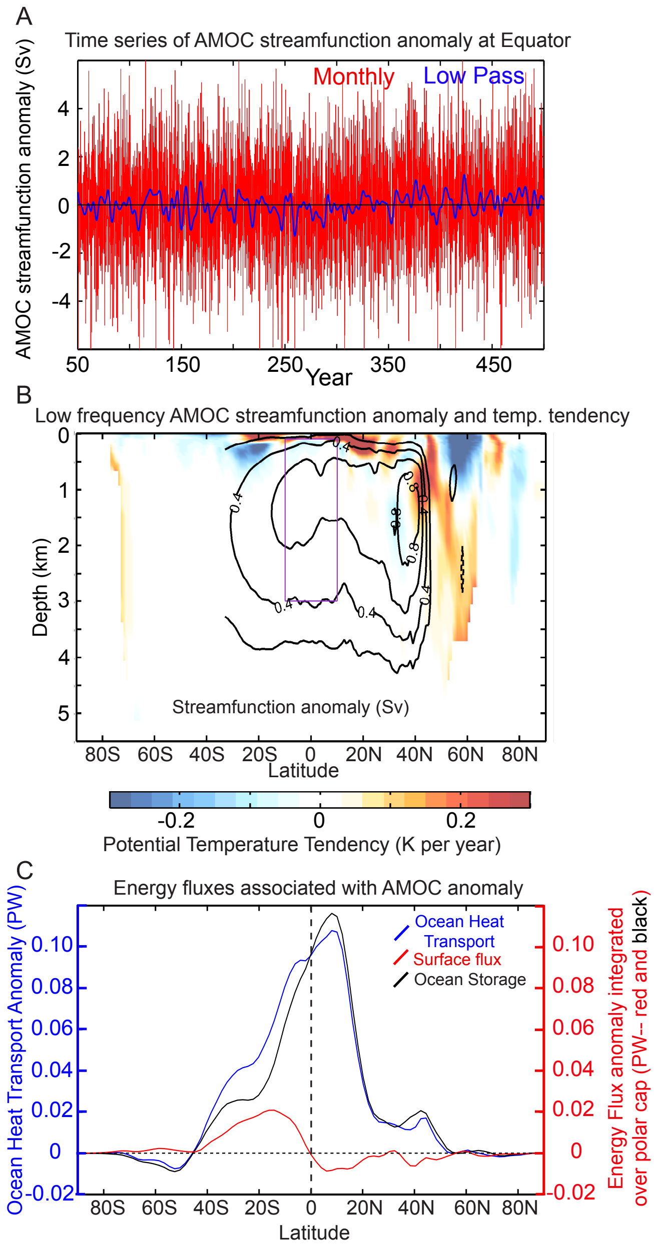

FIG. 7. (A) Time series of AMOC index, defined as the streamfunction anomaly averaged between 100m and 300m depth and between 10°S and 10°N. The red lines are the monthly means and the blue lines are the low pass filtered time series using a cutoff period of 6 years. (B) The contours show the cross section of low-pass AMOC index regressed onto AMOC streamfunction anomaly in Sverdrups. The colored field is the associated temperature tendency in units of Kelvin per year. The purple box shows the region used to define the AMOC index. (C) The ocean meridional heat transport anomaly associated with a 1 standard deviation AMOC event (blue line). The red line is the spatial integral of the surface heat flux (positive to the atmosphere) integrated over the polar cap North of a given latitude and the black line is the storage in the ocean integrated over the polar cap. By construction, the surface flux (red) and the storage (black) sum to the ocean heat transport into the polar cap (blue). The results have been integrated over all ocean basins.

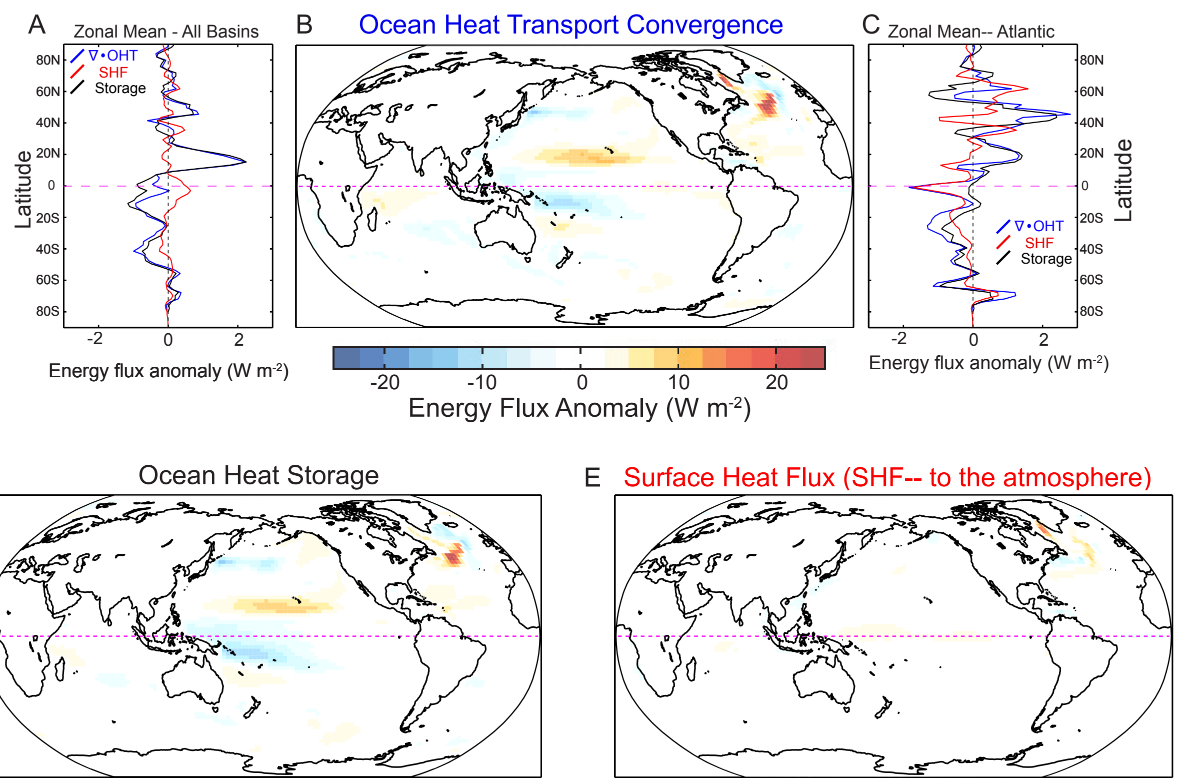

FIG. 8. Spatial maps of anomalies in ocean heat transport convergence (B), column integrated ocean heat content tendency (D – ocean heat storage) and surface heat flux to the atmosphere (E) associated with a 1 standard deviation in AMOC index. Panel (A) shows the zonal means of the anomalies in the ocean heat transport convergence(blue), ocean heat storage (black) and surface heat flux to the atmosphere (red). Panel (C) shows the zonal mean over the Atlantic basin only.

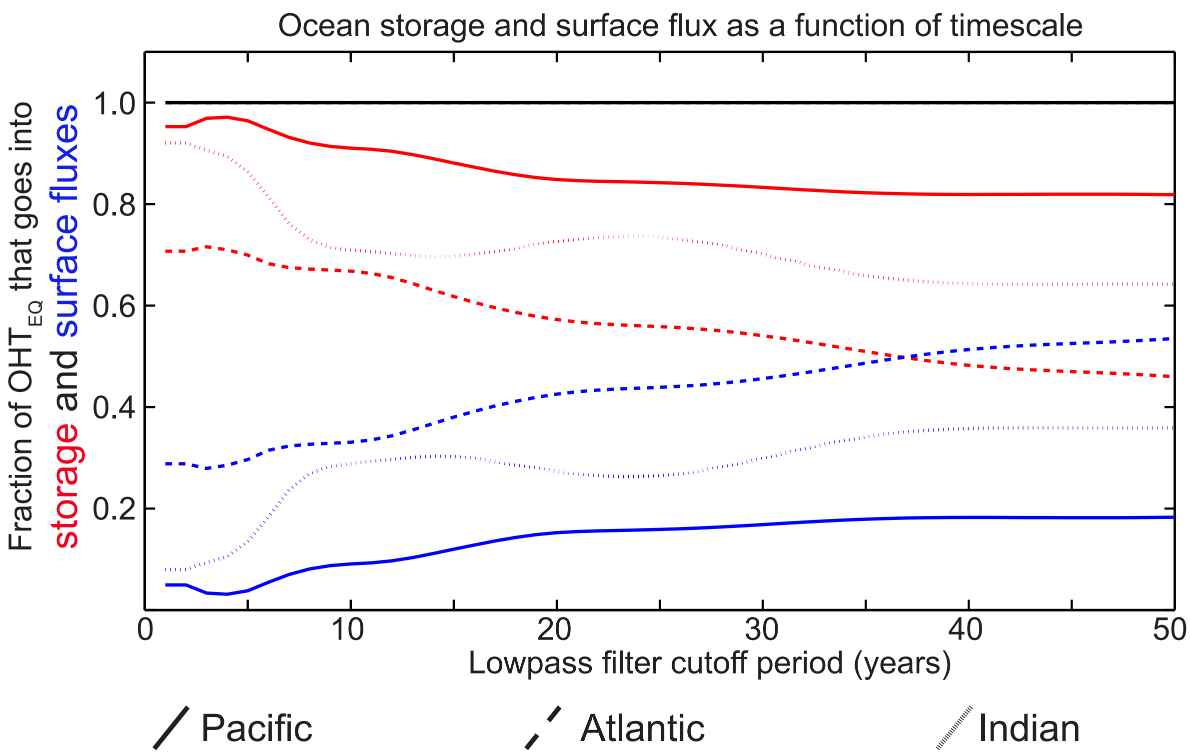

FIG. 9. The fraction of OHT_{EQ} that get stored in the ocean column (red) and fluxed upward to the atmosphere (blue) over the spatial integral of the polar cap as a function of lowpass filter cutoff period. The solid line is for the Pacific basin. The horizontally hashed line is for the Atlantic and the vertically hashed line is for the Indian ocean.